Journal of Magnetic Resonance 200 (2009) 126–129

Contents lists available at ScienceDirect

Journal of Magnetic Resonance

journal homepage: www.elsevier.com/locate/jmr

Selective detection of ordered sodium signals by a jump-and-return pulse sequence

Jae-Seung Lee [a,b], Ravinder R. Regatte [b], Alexej Jerschow [a,*]

[a] Department of Chemistry, New York University, New York, NY 10003, USA
[b] Radiology Department, Center for Biomedical Imaging, New York University School of Medicine, New York, NY 10003, USA

ARTICLE INFO

Article history:
Received 24 April 2009
Revised 18 June 2009
Available online 25 June 2009

Keywords:
Na MRI
MRI contrast
Quadrupolar
Jump-and-return
Pf1 bacteriophage

ABSTRACT

A simple pulse sequence, derived from the shaped pulse optimally exciting the central transition of a spin 3/2, can be used to selectively detect ordered sodium with a given quadrupolar coupling. The pulse sequence consists of two pulses with opposite phases and separated by a delay, called a quadrupolar jump-and-return (QJR) sequence. This QJR sequence is tested with a phantom made of sodium ions in bacteriophage and in aqueous solution and its feasibility for contrast modification based on the quadrupolar coupling is demonstrated.

1. Introduction

A variety of tissues and organs, including the brain, cartilage, the disc, breast, and kidneys, have a large amount of sodium, which makes ^{23}Na MRI a very promising tool for the diagnosis of some important diseases such as osteoarthritis (OA), degenerative disc diseases (DDD), breast cancer, and brain tumors [1–4]. While both free and ordered sodium ions are prevailing throughout the body, monitoring the levels of the latter is of particular interest due to possible correlations between the concentration of the ordered sodium ions and the early symptoms of some disorders [5–11]. In cartilage tissue, for example, the concentration of the sodium ions is particularly high, and they are attracted by the negative charge of glycosaminoglycans (GAGs), a decrease of which is generally a sign for the onset of disorder. Hence, the sodium concentration in the cartilage can be a direct reporter of degenerative joint diseases such as OA and DDD. Techniques for modifying ^{23}Na contrast have been developed in order to cleanly separate ordered sodium ions (in cartilage) from free sodium ions (in non-cartilage tissues) on high-resolution ^{23}Na images both in vivo and ex vivo [12,13,15,14]. In a recent communication, we presented a new ^{23}Na contrast based on a pulse sequence optimally exciting the central peak of ordered sodium ions [16]. Since the goal of singling out the central transition requires the presence of a quadrupolar interaction, the same procedure can be used for the spectral selection of nuclei that experience a quadrupolar interaction. This approach is presented here.

2. Method

Recently, we found that a simple pulse sequence consisting of two pulses with opposite phases and separated by a delay can enhance the signal intensity of the central transition of a spin 3/2, simultaneously suppressing the satellite transitions [16]. This sequence was found by the implementation of an optimal control algorithm [17–22] with the target function chosen such that the central transition is optimized. The pulse sequence obtained via this optimization in an iterative procedure resembled a hard pulse sequence of the form

$$(-\alpha)_y - \tau - \alpha_y, \tag{1}$$

where α is the flip angle of the pulses in radians and y indicates the phase of the pulses. We are going to call this pulse sequence as a quadrupolar jump-and-return (QJR) sequence, drawing on the analogy with commonly-known water suppression techniques [23,24]. Intuitively, one may interpret such a sequence as one that leaves the signal in place if no other interaction is present (chemical shift, dipolar coupling, quadrupolar coupling), since in such a case the second pulse cancels the action of the first. There is a notable distinction in the quadrupolar case, where this approach dictates the use of off-90 degree flip angles for optimal excitation as shown below.

In the presence of a quadrupolar interaction, the intensities of the central and satellite peaks and the x component of the magnetization after applying the QJR sequence (1) to the thermal equilibrium state are

$$I_{\text{center}} = \frac{9}{5}\sin^3\alpha\cos\alpha\sin^2(\pi f_Q\tau), \tag{2}$$

$$I_{\text{satellites}} = \frac{3}{5}\sin\alpha\cos\alpha(3\cos^2\alpha - 1)\sin^2(\pi f_Q\tau), \tag{3}$$

* Corresponding author. Fax: +1 212 260 7905.
E-mail address: alexej.jerschow@nyu.edu (A. Jerschow).

1090-7807/$ - see front matter © 2009 Elsevier Inc. All rights reserved.
doi:10.1016/j.jmr.2009.06.015

and

$$I_x = \frac{6}{5}\sin\alpha\cos\alpha\sin^2(\pi f_Q \tau), \quad (4)$$

where f_Q is the quadrupolar splitting in Hz and $I_{\text{satellites}}$ is the sum of the intensities of the two satellite transitions.

For a given quadrupolar splitting f_Q, we can achieve the maximum intensities when the delay τ is $(2n-1)/(2f_Q)$, where $n = 1, 2, 3, \ldots$. When τ is set to one of these values, I_{center} can reach its maximum value of $27\sqrt{3}/80 \doteq 0.5846$ when $\alpha = \pi/3$, which is very close to the theoretical maximum value of 0.6 [16]. At the same time, the intensity of the satellite transitions is $I_{\text{satellites}} = -3\sqrt{3}/80$, which is 1/9 of I_{center} in terms of the absolute values. Perfect suppression of the satellite transitions ($I_{\text{satellites}} = 0$) can be achieved when $\alpha = \cos^{-1}(1/\sqrt{3}) \approx 54.7^\circ$, which is the magic angle. At the same time, $I_{\text{center}} = 2\sqrt{2}/5 \doteq 0.5657$.

From Eqs. (2) and (3) it is recognized that both the central and satellite peaks will vanish if $f_Q\tau = 0, 1, 2, \cdots$. This result can be expected directly from the QJR sequence itself. As seen in (1), the QJR sequence contains two pulses with opposite phases. If there is no net evolution during the delay between the two pulses, the second pulse will return the magnetization back to the original position. This will happen when the delay τ is set to the multiples of $1/f_Q$ or when $f_Q = 0$. Therefore, the QJR sequence could, for example, serve as a good MRI contrast to discriminate free and ordered sodium ions in tissue by suppressing the signal from free sodium ions and exciting only the central peak of the ordered sodium ions.

3. Experimental

The above idea was tested with a sample consisting of filamentous Pf1 bacteriophage and NaCl aqueous solution. The original Pf1 bacteriophage (ASLA Biotech) with its concentration 53 ± 4 mg/ml was diluted to 15 ± 1 mg/ml by adding phosphate buffered saline solution (Aldrich, pH 7.4). After dilution, the concentration of sodium ions in Pf1 bacteriophage was measured to be 70 mM by comparing its ^{23}Na NMR signal with 50 mM NaCl aqueous solutions. The Pf1 and NaCl solutions were put into 3 mm and 5 mm NMR tubes, respectively, and the 3 mm NMR tube was located inside the 5 mm NMR tube separated by a spacer. The inner and outer diameters of the 3 mm NMR tube were measured as 2.2 mm and 2.9 mm, and those of the 5 mm NMR tube were 4.0 mm and 4.9 mm. The quadrupolar splitting f_Q of ^{23}Na ions in the Pf1 solution was independently measured to be 205 Hz. All the experiments were performed on a Bruker Avance 500 MHz spectrometer.

The sequences for 2D ^{23}Na MRI experiments are shown in Fig. 1. Fig. 1(a) shows the conventional imaging sequence with the system excited by a 90° hard pulse. Fig. 1(b) shows the imaging sequence combined with the QJR sequence. Two refocusing 180° hard pulses are inserted during the delay in the QJR sequence to compensate the chemical shifts differences. For the imaging experiment of Fig. 1(a), the pulse durations were 7.63 μs and 15.25 μs for the 90° and 180° pulses, respectively. The number of scans was 200, and the repetition time between scans was 0.5 s. The echo time (TE) was 5.0 ms. The spectral width was 90.090 kHz, and 1024 data points were acquired. The strength of the gradient pulses was 0.104 T/m for frequency encoding direction and 0.0832 T/m for the phase encoding direction. The number of phase encoding steps was 64. The field of view (FOV) was 76.9 mm × 6.8 mm and the size of a pixel was 0.15 mm × 0.21 mm, respectively. For the imaging experiment with the QJR sequence (Fig. 1(b)), the pulse duration for 54.7° pulse was 4.63 μs. Other experimental parameters were the same as in the experiment of Fig. 1(a).

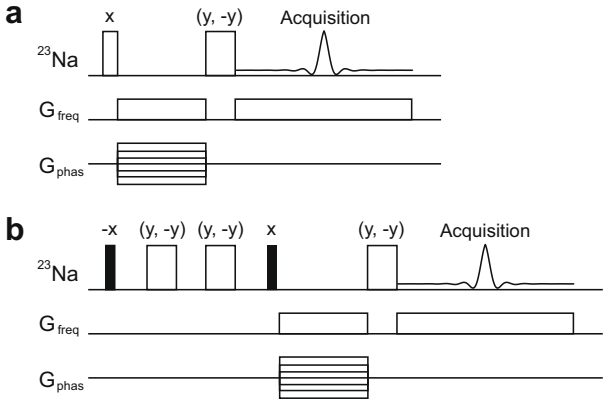

Fig. 1. Pulse sequences for 2D ^{23}Na MRI. In the rf channel, white broad, white, and black thin rectangles represent 180°, 90°, and 54.7° pulses, respectively. The relative phases of the pulses are indicated on top of the rectangles. Paired phases mean that the phases for those pulses were alternated while the phases of the other pulses were not changed. The channels G_{freq} and G_{phas} represent the gradient channels for the frequency and phase encoding, respectively. Two sequences are used for the signal excitation: (a) a sequence of a single 90° pulse and (b) the QJR sequence with the chemical shifts refocused by two 180° pulses.

4. Results and discussion

The results of 2D ^{23}Na MRI experiments are presented in Fig. 2. Fig. 2(a) is the image when the signal is excited by a hard 90° pulse and TE = 5.0 ms, which was about $1/f_Q$ and chosen to avoid the signal decrease due to the evolution by quadrupolar coupling. The image reveals both the inner and outer sample regions. Fig. 2(b) is the image when the signal is excited by the QJR sequence with the delay of 2.5 ms and TE = 5 ms, which shows only the inner tube filled with Pf1 bacteriophage solution.

In Fig. 2, the intensities were normalized with respect to the maximum intensity of the image obtained with a hard 90° pulse, which comes from the outer region of Fig. 2(a). The maximum intensity from the inner region of Fig. 2(a) was about 0.76, and that from the image in Fig. 2(b) was about 0.47. The ratio of these values is 0.62, which is somewhat larger than the expected value of 0.5657 because the satellite peaks ($T_2 \sim 18$ ms) decay faster than the central peak ($T_2 \sim 35$ ms) during the spin-echo imaging sequence.

The analysis of the QJR sequence in Eqs. (2)–(4) assumed perfect rotations by the rf pulses, which may not be possible in a real experiment due to the finite duration and rf amplitude of the pulses. If the pulses are not strong compared to f_Q, numerical simulations show that the intensity of the central peak I_{center} can still be made larger than 0.58, which is more than 96% of the theoretical maximum, by adjusting the delay between the pulses (Fig. 3). The delay needed to maximally excite the central transition becomes shorter with the rf amplitude of the pulses decreased or the duration of the pulses increased. The total duration of the QJR sequence, which is the sum of the pulse durations and delay, becomes longer at the same time.

The density matrix of the central peak is an eigenvector of the quadrupolar Hamiltonian $\mathcal{H}_Q = \pi f_Q\left[I_z^2 - I(I+1)\right]$, as well as, the Redfield matrix of quadrupolar relaxation (see Eq. (10) of Ref. [25]). Therefore, once we excite the central peak and suppress the satellite peaks, the satellite peaks would not appear during our imaging experiment (Fig. 1(b)). This feature makes the QJR sequence more favorable for MRI than other ^{23}Na contrast methods, such as the inversion recovery (IR) [14] and quadrupolar filter by nutation (QFN) [15], which excite both the central and satellite peaks. On the other hand, the QJR sequence rather selects a narrow range of the quadrupolar coupling constants, compared with the IR

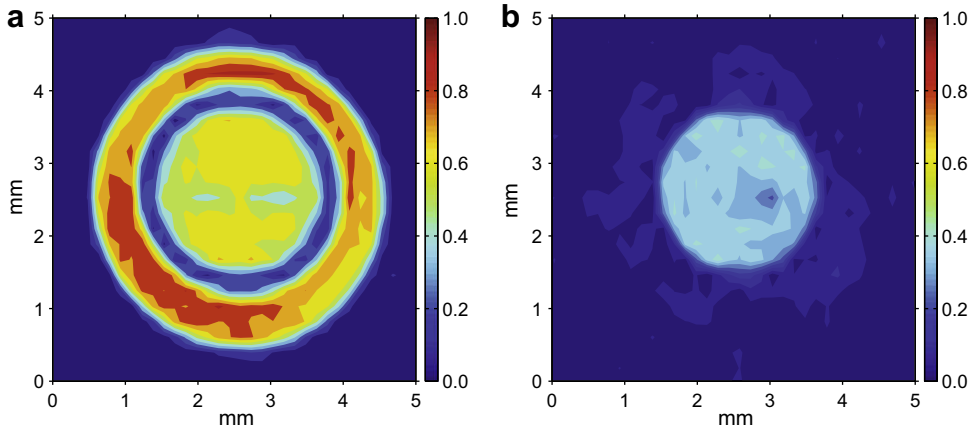

Fig. 2. 2D ^{23}Na images obtained with the pulse sequences shown in Fig. 1. (a) The signal is excited by a hard 90° pulse. (b) The QJR sequence with a delay of 2.5 ms was used to excite the signal. The phantom consists of two concentric tubes (3 mm and 5 mm od, respectively), the inner tube filled with Pf1 bacteriophage solution and an outer with 50 mM NaCl solution.

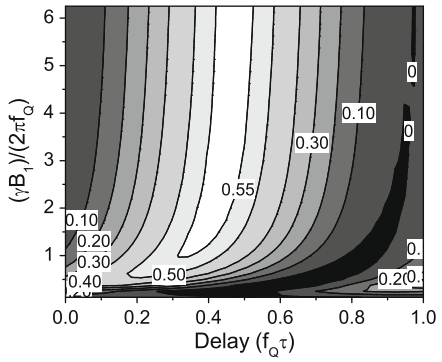

Fig. 3. Intensity of the central peak as a function of the delay and the rf amplitude of the pulses in the QJR sequence. The pulse flip angle was fixed to 54.7°, so the pulse duration was determined according to the rf amplitude. The quadrupolar coupling was included when evaluating the evolution during the pulses.

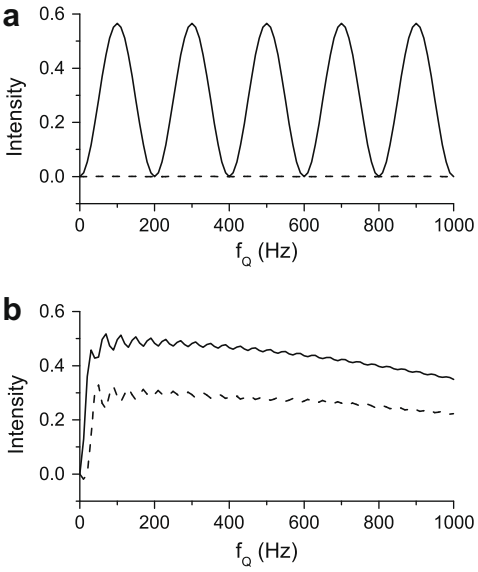

Fig. 4. Comparison of the QJR and QFN sequences. Solid and dashed lines are the intensities of the central and satellite peaks, respectively. (a) Performance of the QJR sequence consisting of two 54.7° pulses with $\gamma B_1 = 2\pi \times 1000\ s^{-1}$ and a delay of 5 ms. (b) Performance of the QFN sequence consisting of a 25 ms soft 90° pulse and a 250 μs hard 90° pulse.

and QFN methods (see Fig. 4). Furthermore, we would like to emphasize that a similar approach should be possible with any bilinear Hamiltonian (scalar coupling, dipolar coupling), although the issues specific to the central vs. satellite transitions are only relevant to odd spin values (such as the case of three coupled spins 1/2, for example).

5. Conclusion

We described here a quadrupolar jump-and-return sequence as a quadrupolar selection pulse sequence for a spin 3/2, in particular ^{23}Na, to distinguish between free and ordered sodium ions. It does not excite the signals from free sodium ions, and for the ordered ones, suppresses the satellite peaks and enhances the central peak. The sequence was born to life originally through an optimal control optimization scheme, but the result appears to be a particularly simple approach which does not require the implementation of shaped rf pulses. The QJR sequence may extend the use of ^{23}Na MRI as a diagnostic tool, but similar approaches may also find applications in spin-1/2 NMR/MRI.

Acknowledgments

We acknowledge funding from the Bayer HealthCare Pharmaceuticals, as well as, from the US National Science Foundation under Grant No. 0554400.

References

[1] T. Shimizu, H. Naritomi, T. Sawada, Sequential changes on ^{23}Na MRI after cerebral infarction, Neuroradiology 35 (1993) 416–419.
[2] A. Bashir, M.L. Gray, J. Hartke, D. Burstein, Nondestructive imaging of human cartilage glycosaminoglycan concentration by MRI, Magn. Reson. Med. 41 (1999) 857–865.
[3] R. Ouwerkerk, M.A. Jacobs, K.J. Macura, A.C. Wolff, V. Stearns, S.D. Mezban, N.F. Khouri, D.A. Bluemke, P.A. Bottomley, Elevated tissue sodium concentration in malignant breast lesions detected with non-invasive ^{23}Na MRI, Breast Cancer Res. Treat. 106 (2007) 151–160.
[4] M. Nimrod, R. Yael, R.H. Glenn, I. Alex, N. Long, L.E. Robert, Sodium MRI of the human kidney at 3 Tesla, Magn. Reson. Med. 56 (2006) 1229–1234.
[5] E. Shapiro, A. Borthakur, A. Gougoutas, R. Reddy, Na-23 MRI accurately measures fixed charge density in articular cartilage, Magn. Reson. Med. 47 (2002) 284–291.
[6] A. Borthakur, E. Shapiro, J. Beers, S. Kudchodkar, J. Kneeland, R. Reddy, Sensitivity of MRI to proteoglycan depletion in cartilage: comparison of sodium and proton MRI, Osteoarthritis Cartilage 8 (2000) 288–293.
[7] A. Wheaton, A. Borthakur, G. Dodge, B. Kneeland, H. Schumacher, R. Reddy, Sodium magnetic resonance imaging of proteoglycan depletion in an in vivo model of osteoarthritis, Acad. Radiol. 11 (2004) 21–28.

[8] A. Wheaton, A. Borthakur, E. Shapiro, R. Regatte, S. Akella, J. Kneeland, R. Reddy, Proteoglycan loss in human knee cartilage: quantification with sodium MR imaging—feasibility study, Radiology 231 (2004) 900–905.
[9] A. Borthakur, E. Shapiro, S. Akella, A. Gougoutas, J. Kneeland, R. Reddy, Quantifying sodium in the human wrist in vivo by using MR imaging, Radiology 224 (2002) 598–602.
[10] E. Insko, D. Clayton, M. Elliott, In vivo sodium MR imaging of the intervertebral disk at 4 T, Acad. Radiol. 9 (2002) 800–804.
[11] R. Reddy, E. Insko, E. Noyszewski, R. Dandora, J. Kneeland, J. Leigh, Sodium MRI of human articular cartilage in vivo, Magn. Reson. Med. 39 (1998) 697–701.
[12] R. Kemp-Harper, S. Brown, C. Hughes, P. Styles, S. Wimperis, ^{23}Na NMR methods for selective observation of sodium ions in ordered environments, Prog. Nucl. Magn. Reson. Spectrosc. 30 (1997) 157–181.
[13] G. Navon, H. Shinar, U. Eliav, Y. Seo, Multiquantum filters and order in tissues, NMR Biomed. 14 (2001) 112–132.
[14] P. Rong, R.R. Regatte, A. Jerschow, Clean demarcation of cartilage tissue ^{23}Na by inversion recovery, J. Magn. Reson. 193 (2008) 207–209.
[15] J. Choy, W. Ling, A. Jerschow, Selective detection of ordered sodium signals via the central transition, J. Magn. Reson. 180 (2006) 105–109.
[16] J.-S. Lee, R.R. Regatte, A. Jerschow, Optimal nuclear magnetic resonance excitation schemes for the central transition of a spin 3/2 in the presence of residual quadrupolar coupling, J. Chem. Phys. (2008) 224510-1–224510-6.
[17] T.E. Skinner, T.O. Reiss, B. Luy, N. Khaneja, S.J. Glaser, Application of optimal control theory to the design of broadband excitation pulses for high-resolution NMR, J. Magn. Reson. 163 (2003) 8–15.
[18] N. Khaneja, T. Reiss, C. Kehlet, T. Schulte-Herbruggen, S.J. Glaser, Optimal control of coupled spin dynamics: design of NMR pulse sequences by gradient ascent algorithms, J. Magn. Reson. 172 (2005) 296–305.
[19] N.I. Gershenzon, K. Kobzar, B. Luy, S.J. Glaser, T.E. Skinner, Optimal control design of excitation pulses that accommodate relaxation, J. Magn. Reson. 188 (2007) 330–336.
[20] N. Khaneja, B. Luy, S.J. Glaser, Boundary of quantum evolution under decoherence, Proc. Natl. Acad. Sci. USA 100 (2003) 13162–13166.
[21] N. Khaneja, J.-S. Li, C. Kehlet, B. Luy, S.J. Glaser, Broadband relaxation-optimized polarization transfer in magnetic resonance, Proc. Natl. Acad. Sci. USA 101 (2004) 14742–14747.
[22] T. Vosegaard, C. Kehlet, N. Khaneja, S.J. Glaser, N. Chr. Nielsen, Improved excitation schemes for multiple-quantum magic-angle spinning for quadrupolar nuclei designed using optimal control theory, J. Am. Chem. Soc. 127 (2005) 13768–13769.
[23] P. Plateau, M. Guéron, Exchangeable proton NMR without baseline distortion, using new strong-pulse sequences, J. Am. Chem. Soc. 104 (1982) 7310–7311.
[24] H. Bleich, J. Wilde, Solvent resonance suppression using a sequence of strong pulses, J. Magn. Reson. 56 (1984) 154–155.
[25] G. Jaccard, S. Wimperis, G. Boddenhausen, Multiple-quantum NMR spectroscopy of $S = 3/2$ spins in isotropic phase: a new probe for multiexponential relaxation, J. Chem. Phys. 85 (1986) 6282–6293.